PLANFORM OF GLOBAL MANTLE CONVECTION PATTERN FOR VENUS; R.R. Herrick, and R.J. Phillips, Dept. of Geological Sciences, Southern Methodist University, Dallas, TX 75275

Introduction. Recent work (1,2) has suggested that, for a fairly robust set of conditions, the pattern of mantle convection for an Earth-sized planet should be that of isolated upwellings amidst an interconnected network of sheetlike downwellings. Because it has been argued that long-wavelength topography on Venus reflects, at least in part, the effects of mantle convection (3), this planet may be an ideal place to examine this concept despite the lack of seismic information. We have tested this idea by constructing a model that assumes that the Venusian long-wavelength topography and gravitational potential are caused by density anomalies due to convection and near-surface effects. Near-surface effects may include crustal thickness variations, lithospheric density or temperature anomalies, etc., but will hereafter be lumped into the term "crustal thickening". At the long wavelengths used, near-surface effects cannot be resolved from one another with the available data. Using inversion techniques, we have transformed spherical harmonic models of the Venusian topography (4) and gravitational potential (5) into global maps of crustal thickening and the mantle convection pattern. These maps can be used further to identify large-scale topographic features that are dynamically maintained.

Procedure. Crustal thickening can be represented by variations in surface density on a spherical shell located at the mean depth of the base of the crust (assumed to be 15 km below mean planetary radius (6)). Assuming Airy isostasy, a simple linear relationship exists between the spherical harmonic coefficients (SHCs) of the crustal shell and those of the resulting topography and potential (7). For the potential this relationship is different for each spherical harmonic degree. A crustal density of 2900 kg/m^3 was assumed.

Most of the contribution to dynamically supported topography and geoid signals comes from density structure due to mantle temperature anomalies associated with the upper boundary layer of convection (8). Thus we represent mantle contribution to the geoid and topography by a second shell of varying surface density placed at an appropriate depth in the upper mantle. In the calculations a depth of 200 km was used. We follow previous work (9,10) that has solved simplified forms of the Navier-Stokes equations to develop equations for kernels that relate the SHCs of the shell to the surface gravitational potential and the geoid to topography ratio. The model assumes that the mantle is a Newtonian, incompressible viscous fluid. The core is assumed to be inviscid and a free-slip condition is used at the core-mantle boundary. The core was assigned a radius of 3300 km and a density of 9900 kg/m^3. The mantle was assumed to be isoviscous with a viscosity of 1.0×10^{21} Pa s and was assigned a density of 4400 kg/m^3. A value of 8.87 m/s^2 was used for gravitational acceleration throughout the mantle. The calculated kernels were used to develop a linear relationship between the SHCs of the mantle shell and the SHCs of the topography and potential field. This relationship is different for each spherical harmonic degree.

The result is that for each spherical harmonic degree a 2 x 2 matrix relates the two SHCs of the surface density shells to the SHCs of the topographic and potential fields. We inverted each of these matrices and multiplied by the SHCs of the topography and gravitational potential to calculate the SHCs for the crustal thickening and mantle convection shells. A 5 x 5 degree grid spacing was used to produce the global maps to degree and order 10 of crustal thickening and upper mantle density pattern shown in Figures 1 and 2. The mantle convection shell was then forward transformed to produce SHCs for only the dynamic contribution

to the topographic field. This is shown in Figure 3 with the total topography to degree and order 10 shown in Figure 4 for comparison. The crustal thickening contribution to topography can be found by dividing the values in Figure 1 by the negative of the crustal density.

Discussion. The mantle flow field has a pattern of isolated upwellings (unshaded) amidst an interconnected network of downwellings in reasonably good agreement with the predictions of (1) and (2). Figure 3 shows that the only large-scale, high-elevation features that are predicted to be primarily dynamically supported are Thetis (-20N, 130E), Atla (0N, 195E) and Beta (30N, 280E) Regiones. Figure 1 shows that Ovda Regio (-5N, 90E) and Ishtar Terra (70N, 0E), for example, appear to be supported primarily by near-surface effects.

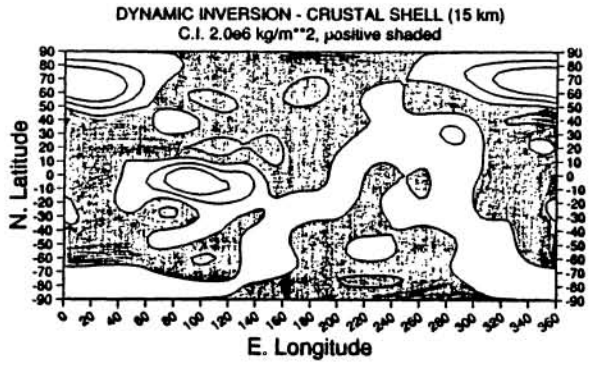

Figure 1

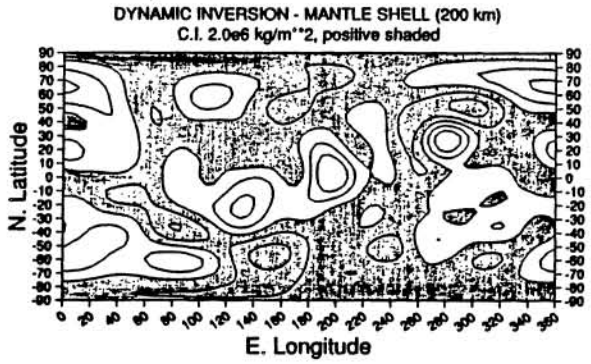

Figure 2

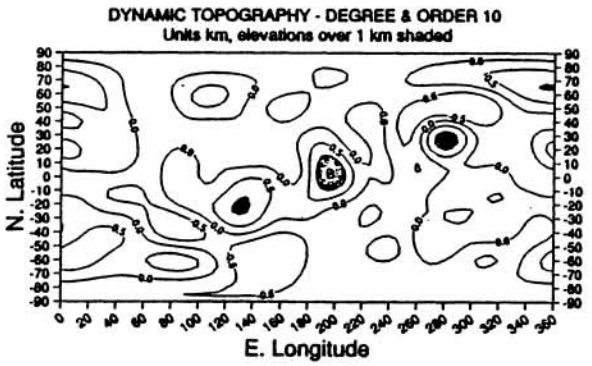

Figure 3

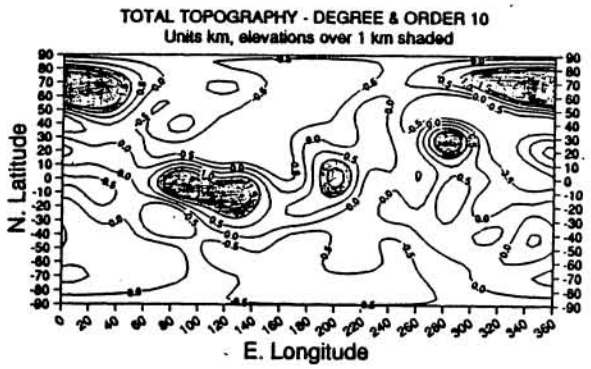

Figure 4

References. (1) Bercovici, D., *et al.*, 1989, *Science, 244*, 950-955. (2) Bercovici, D., *et al.*, 1989, *GRL, 16*, 617-620. (3) Phillips, R.J., and M. Malin, 1984, *Ann. Rev. Earth Planet. Sci., 12*, 411-443. (4) Bills, B., *et al.*, 1987, *JGR, 92*, 10,335-10,351. (5) Bills, B., and M. Kobrick, 1985, *JGR, 90*, 827-836. (6) Grimm, R., and S. Solomon, 1988, *JGR, 93*, 11,911-11,929. (7) Phillips, R.J., and K. Lambeck, 1980, *Rev. Geophys. Space Phys., 18*, 27-76. (8) Parsons, B., and S. Daly, 1983, *JGR, 88*, 1129-1144. (9) Richards, M. and B. Hager, 1984, *JGR, 89*, 5987-6002. (10) Hager, B., and R. O'Connell, 1981, *JGR, 86*, 4843-4867.